JOURNAL OF MATERIALS SCIENCE 26 (1991) 1910–1918

On the sensitivity of electron channelling line shapes to dislocation distribution

M. KACZOROWSKI*, W. W. GERBERICH
Department of Chemical Engineering and Materials Science, University of Minnesota, Minneapolis, Minnesota 55455 USA

Considerations of the electron channelling pattern formation in a medium consisting of subcells with orientations oscillating in a range, $\alpha \pm \Delta\alpha$, are presented. These are followed by an experiment which compares well with theoretical expectations. It is shown that selected area channelling pattern (SACP) line resolution not only depends on the total density of dislocations but also on their distribution. It is also shown that for a given dislocation density, the degradation of SACPs is more pronounced for a random distribution than for one with a subcell structure. The arrangement of the dislocations into subcells make the body a two-component medium in which the undeformed spaces are penetrated by a high density dislocation array forming a three-dimensional network of subcell walls. This kind of structure will generate an SACP which is a superposition of relatively undeformed channelling patterns. These are shifted each from the other by an angle α which is a function of subcell misorientation. The increase in the width of SACP-lines is mostly influenced by the value of $\pm \Delta\alpha$ which can be considered as a scattering band for an average subcell misorientation typical for a given dislocation density.

1. Introduction

Since 1967, when the electron channelling phenomenon was discovered by Coates [1], many attempts have been made to make this technique a useful tool for practical purposes. These have been connected with electron channelling patterns (ECPs) as a probe of both orientation and structure either from the point of view of symmetry or "quality". The last one concerns both elastic [2] or plastic [3–5] deformation caused by different arrangements of defect clusters and dislocations. One major thrust, useful in deformation and fracture studies, has been to quantify the dislocation density in metallic crystals. The first qualitative studies have been followed by quantitative attempts to find a relationship between ECP line width and the degree of deformation. The earliest by Stickler and coworkers [6] evaluated the pattern quality simply by comparing the angular width of the finest line visible anywhere on the ECP to the strain applied. Despite the choice of the line being an arbitrary one, many studies have confirmed a good correlation between the bulk deformation [7, 8] and this quantity. The strain can even be assessed by visual comparison of the experimental pattern to a calibrated sequence of ECPs obtained at different applied strains [9]. By using the finest line width method, Gerberich *et al.* [10] proposed a very simple relationship between ECP-line resolution and deformation.

It should be mentioned, however, that in these experiments, which often were performed on single crystals deformed in tension or compression, it was tacitly assumed that the distribution of dislocations was random. This assumption will not persist in many cases. For example, it does not appear to be the case when low energy subcell configurations are formed. Here it is well known during cyclic loading that only a part of the space is occupied by densely packed dislocation walls, while the interior of the subcells are nearly dislocation free. It follows that the whole space can be considered as the superposition of a three-dimensional, highly strained mesh and undeformed regions. In turn, these "undeformed" regions have slightly different crystallographic orientations with respect to each other. This type of structure would appear to have a different influence on the degradation of ECP lines compared to the random dislocation arrangement that had been originally envisioned by Stickler and collaborators [6].

2. Theoretical considerations

"Electron channelling patterns are caused by a variation of the signal resulting from changes in the angle between the incident beam and the crystal lattice of the specimen" [11]. Consider the case for a 10 μm diameter area, which is easily sampled using the selected area channelling pattern (SACP) technique. If this area consists of only two subregions misoriented by an angle α as indicated in Fig. 1a, then Fig. 1b schematically shows how this will change the total intensity

* *Permanent address*: Institute of Forming and Casting, the Technical University of Warsaw, ul. Narbutta 85, 02-524 Warsaw, Poland.

0022–2461/91 $03.00 + .12

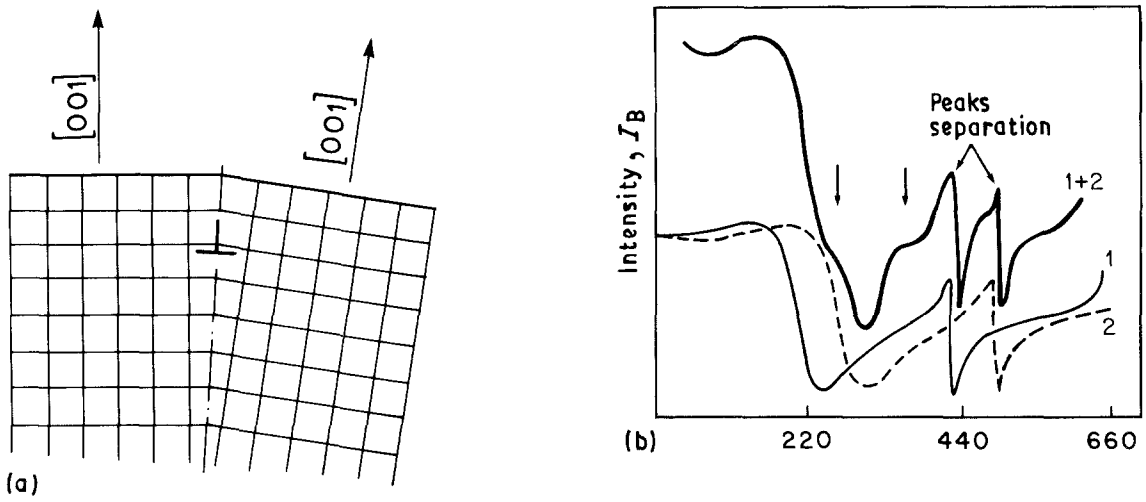

Figure 1 Sketch illustrating (a) geometry and (b) intensity distribution of backscattered electrons for two subregions tilted at an angle α each to the other.

distribution across 200-type bands. For this purpose, theoretical curves for silicon, as presented by Hirsch and Humphreys [12], are superposed. It is easily seen for this simple situation that there is only a relatively small change of line shape in the total intensity curve at the places indicated by arrows. For much larger differences in orientation, e.g. a few degrees, one could expect the separation of the ECP poles.

In reality, the situation is more complicated because the typical subcell size is approximately 1 μm which means that the area sampled consists of many cells. Theoretically, each of an array of such subcells might have a different orientation but practically, because of many constraints, they oscillate in some regime. First of all, one grain will tend to have a single orientation on the average. It follows then that the sum of all subcell misorientations should be equal to zero in the absence of strain gradients. Secondly, for a given strain, there is a characteristic density of dislocations which are concentrated in the cell walls and the distance, l_s, between individual dislocations is a function of that density [13]. At a given deformation, that distance l_s can be assumed to be constant, which means that the misorientation angle α is also constant since $\alpha = b/l_s$, where b is Burger's vector. Throughout such a grain the population will tend to have the same orientation with respect to the electron beam. However, the number of subcells of one orientation can be different from another on a local scale. It follows that the intensity of the backscattered electrons sampling those two sets of subcells will also be different.

Fig. 2a to c show how the total intensity distribution changes for three different populations of two sets of subcells whose constant misorientation causes shifting of the ECP-line intensity. It can be seen that the line shape depends on the ratio between the two populations with the total intensity distribution changing from a single peak with a small inflection into a double-peaked distribution. It is obvious that this shape will also depend on misorientation angle. It should be mentioned that in the first case, the position of the peak, with respect to the minimum, is very different from that for each of the single ones. This may disproportionately increase the measured line width in many cases compared to what would normally be measured for the same dislocation density. In

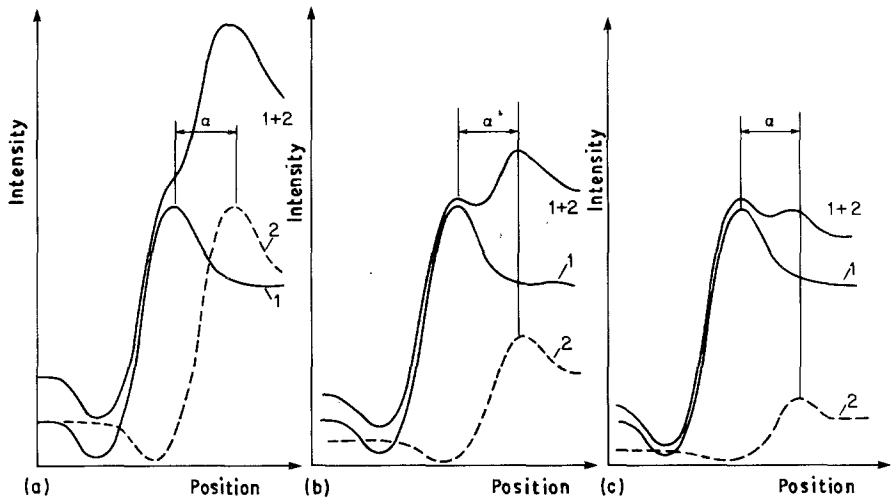

Figure 2 The dependence of the total intensity distribution for an ECP as a function of different populations of two subcell sets for a consistent misorientation angle, α: (1) population 1:1, (b) population 1:2, (c) population 1:4.

the second and the third cases, some "interaction" between the two component peaks can be expected which in time will decrease the distance between the peaks observed on the total curve. Despite this, the separation of peaks is a rough indication of the average misorientation between two or three different subcell sets. It is truly indicative for the case when the subcells are tilted with respect to each other with the axis of rotation being in the plane of the specimen surface. Then, the separation between the peaks is constant and independent of the place in which the measurements have been performed.

The second simple case is where we consider a cross-section through subcells with the axis of rotation being perpendicular to the surace of the sample or parallel to the beam axis. This should represent a rotation between subcells. In that situation, if the position of the pole is assumed to be fixed, the bands on the ECPs will rotate through an angle α. It follows that the position of the peaks will increase with the distance from the "centre" of rotation. To determine the average angle of rotation between two sets of subcells, one would have to measure the splitting of the peaks on a given ECP line minimum at two positions placed at a different distance from the rotation axis. The general situation involving both tilting and rotation needs a thorough consideration of both grain orientation with respect to the optical axis and those possible operating slip systems which provide formation of the subcell walls.

The purpose of the present study was to provide an evaluation of several of the above considerations, that is, how do electron channelling pattern line shapes evolve due to the low energy dislocation configurations and local tilt misorientations associated with fatigue? For that purpose, both thin film TEM and SACP studies of a coarse-grained steel subjected to plastic-strain cycling were conducted.

3. Experimental procedure

The experiment has been performed on a high strength low alloy (HSLA) steel of composition: 0.070 C, 0.51 Mn, 0.03 Si, 0.01 Al and 0.014 Nb wt %. The steel contained an average grain size of 60 μm with a room temperature monotonic yield strength of 210 MPa. The miniature tensile-type specimens had a geometry with a gauge diameter and length of 3 and 10 mm, respectively. Before the experiment, a part of the thread crest was removed in order to fix the position of the sample. In this way, the same position was maintained with regards to the axis of the electron beam. Then the surface of the specimen was electropolished to avoid the influence of microroughness and any surface damage from specimen preparation which might affect the quality of ECP lines. After that, the specimen was observed in a JEOL JSM-840 II scanning electron microscope to select a few grains positioned along the specimen axis. They were then repeatedly investigated after low cycle fatigue loading at a frequency, $f = 0.2$ Hz and $\Delta\varepsilon_p \approx 0.0004$. Since the specimen was basically loaded from zero to tension, this ratchetting-type of low cycle fatigue process produced a gradual, repeated lengthening of the test specimen as well as the grains at the surface. Thus local deformation could also be evaluated by measuring the length of each grain in an orientation parallel to the tension axis. One example of this is shown in Fig. 3a and b. During SEM observations, both topography and selected area channelling patterns were recorded. These were performed using backscattered electrons (BSE) which are sensitive to the crystallographic orientation of the sample. For electron channelling a special SACP attachment was used which allows one to sample an area of 10 μm in diameter or less [14]. The lower bound with the present instrument appears to be on the order of 4 μm [15]. In this mode of observation, the following constant conditions were used

Accelerating voltage	$U = 25$ kV
Working distance	WD = 7 mm
Objective lens aperture	$d = 30$ μm
Rocking angle	$\alpha = \pm 11°$
Beam divergence	$\Delta\alpha = 1 \times 10^{-6}$ rad

It should be noted that all observations were performed for one adjustment of the microscope (SACP). The resolution of ECP lines was measured using microdensitometer traces prepared at a magnification of 20X. The cyclic deformation was continued to an average cumulative strain of $\bar{\varepsilon} = 11.8\%$. Then the sample was sliced into small discs with a thickness of 0.07 mm. These were electropolished for TEM observations using the one-jet polishing method. The TEM study was performed on JEOL 100CX at an accelerating voltage of 100 kV.

4. Results

Both SEM channelling and TEM observations were used to study the deformation process in cyclically loaded HSLA steel. The goal of the first technique was to find whether or not there is an influence of the dislocation distribution on the intensity distribution curve taken across the SACP bands. TEM experiments were then performed to evaluate directly the density of dislocations and their distribution. This later study also provided some information about the size and shape of the subcells and the distance between dislocations in the cell walls.

4.1. SEM observations

First, Fig. 4a and b show an example of a single grain with and without deformation. The corresponding SACPs which had been taken from approximately the same place in the grain marked by the cross on the micrographs, are given in Fig. 4c and d. Although it is easy to ascertain the SACP line degradation with strain, it would be quite difficult to quantify this by using calibration curves presented in the literature. The reason is that the line resolution appeared not to change much but split into several maxima as can be seen on the microdensitometer traces (Fig. 4e and f). These microdensitometer traces have been taken across the same line exactly at the same place. The line resolution is equal to 7.26 mrad for the sample with-

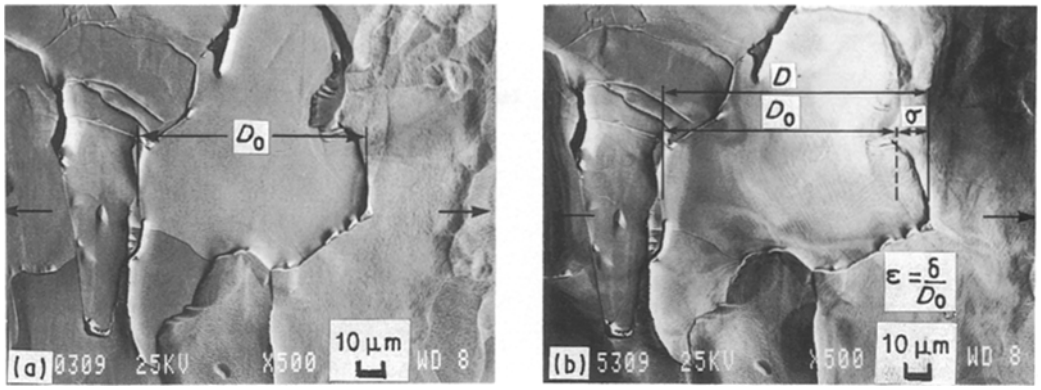

Figure 3 A single grain illustrating the method of evaluating local tensile deformation: (a) single grain without deformation, (b) the same grain after cyclic deformation; note that the specimen tensile axis is parallel to the length markers.

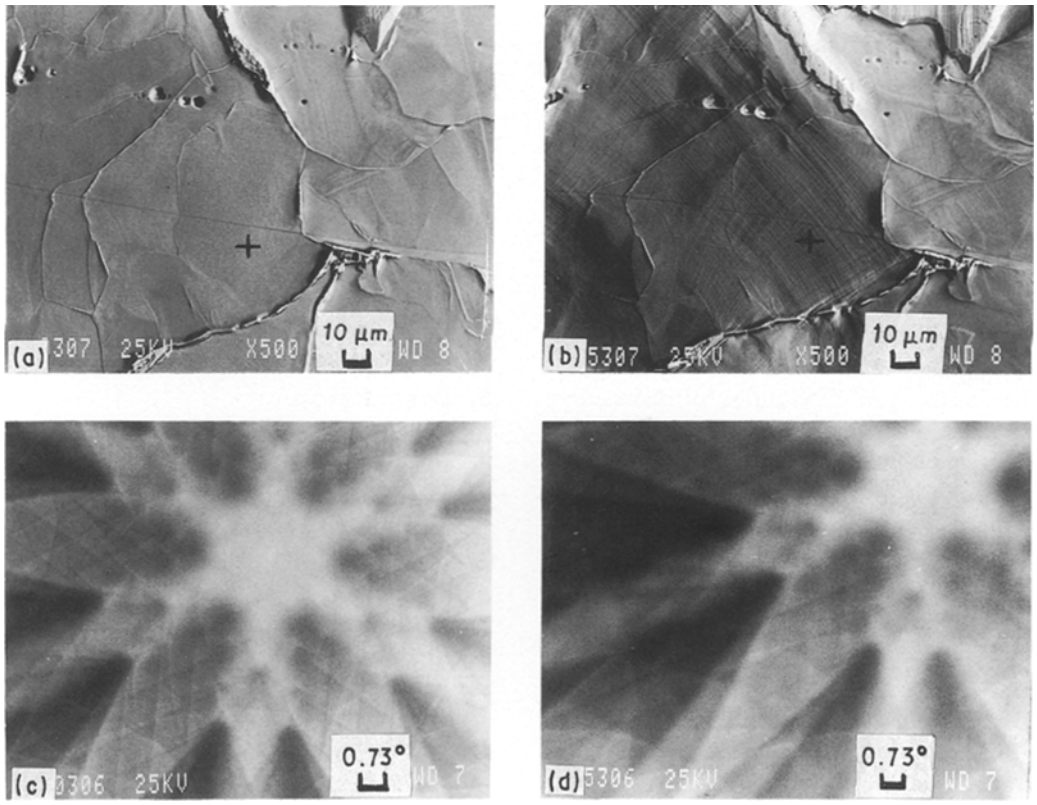

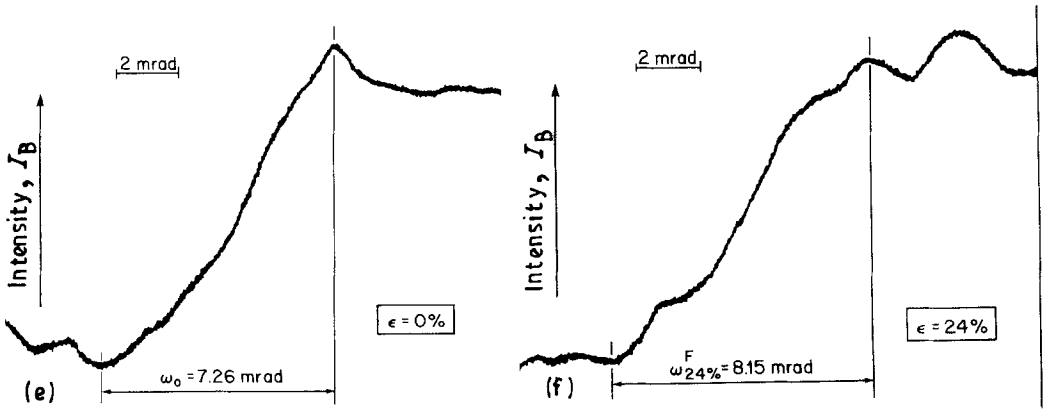

Figure 4 A single grain (a) before and (b) after cycling; (c) and (d) ECPs from these grains before and after deformation and (e) and (f) microdensitometer traces taken at the same place across one of the ECP-lines shown in (c) and (d), respectively.

out deformation and 8.15 mrad after cyclic straining up to $\varepsilon_p = 0.24$. This presents several pertinent points. First, the line resolution for the specimen with no deformation looks suprisingly high. According to the calibration curve presented by Gerberich *et al.* [10], this line width suggests a deformation of $\varepsilon \sim 0.07$. It should be mentioned here however that in the present experiment the finest line was not used but one which was visible on each SACP, thus the use of a "finest-line" calibration would necessarily lead to an over-estimation. The second is the fact that the line resolution did not change much with 24% deformation, that is, the total increase in the SACP-line width of only 12% would represent an incremental strain much less than 24%. Finally, one can distinguish shape changes in the microdensitometer traces upon comparing Fig. 4e and f. As mentioned earlier, there is some splitting into two maxima with additional curvature during the increasing part of the microdensitometer trace. From the separation distance between these two maxima, shown in Fig. 4f, one can determine that in the case of simple tilting, with the axis lying in the surface of the sample, the misorientation between two sets of subcells would be equal to $\sim 0.2°$. This value agrees fairly well with a typical misorientation which is a few tenths of a degree.

4.2. TEM observations

To reiterate, the main reason for the TEM study was to verify the density and distribution of dislocations and also the size of dislocation subcells. The sequence of micrographs presented in Fig. 5 shows the typical dislocation structure in a fatigue sample. It is clear that dislocations are rearranged into subcells elongated mainly in a $\langle 121 \rangle$ direction. The average width of these subcells is 0.8 μm. A few selected area diffraction patterns (SADs) were obtained for this area to check any orientation differences between single subcells. This could not be done with high accuracy because of the relatively small thickness and quite high deformation of the foil, thus, there were no Kikuchi lines and the magnetic properties of the sample made tilting experiments very difficult. Therefore, the position of the sample was kept constant and a number of SAD patterns were obtained for this orientation.

Only in one case was a clear difference in orientation of this subcell set found. These two maximally different SAD patterns are shown in Figs 6a and 6b, while Fig. 6c illustrates the "approximate" geometry for this situation. It follows from the sketch (Fig. 6c) that in such a case the misorientation between subcells would be $\sim 3.6°$. In fact, only one SAD pattern represents an exact two-beam condition and for that reason one can expect the misorientation to be less than 3°, nevertheless, this is still very high. It should be mentioned, however, that among many subcells only one differs so much in orientation with respect to the population which would be sampled during an SACP experiment using a rocking beam spot size of 10 μm in diameter. Thus, its contribution to the SACP is too small to be detectable in the micrograph and, hence, in the microdensitometer trace.

The average dislocation density measured on the basis of a few samples is equal to $8 \times 10^{13}\ m^{-2}$ and the distance between them in the cell wall is about 35 nm. In Fig. 7, one such subcell wall is shown where the dislocations are parallel to each other and the distance is somewhat smaller. It appears also that the centre of the subcells is not always dislocation free. This can be seen in Fig. 8. It follows that depending on the number of "disturbing" dislocations inside the subcell, that these also can influence the SACPs line width.

5. Discussion

First, consider how the above results impact upon the theoretical considerations proposed above. Fig. 9 illustrates a microdensitometer trace obtained by superposition of two original traces for a strain of zero (see Fig. 4e) but of different intensity. Also, they were shifted each with respect to the other. One of these traces (high intensity) is assumed to originate from a population of N_s subcells while the second came from a population of $0.25\ N_s$ subcells. They are shifted by a distance corresponding to 0.25°. The total intensity distribution does not differ too much from that presented in Fig. 4f. Now it is possible to evaluate the angle between subcells in the case of a simple tilt boundary. Recalling that according to Hull [13], for small angles, $\alpha = b/l_s$ (rad) and taking from TEM

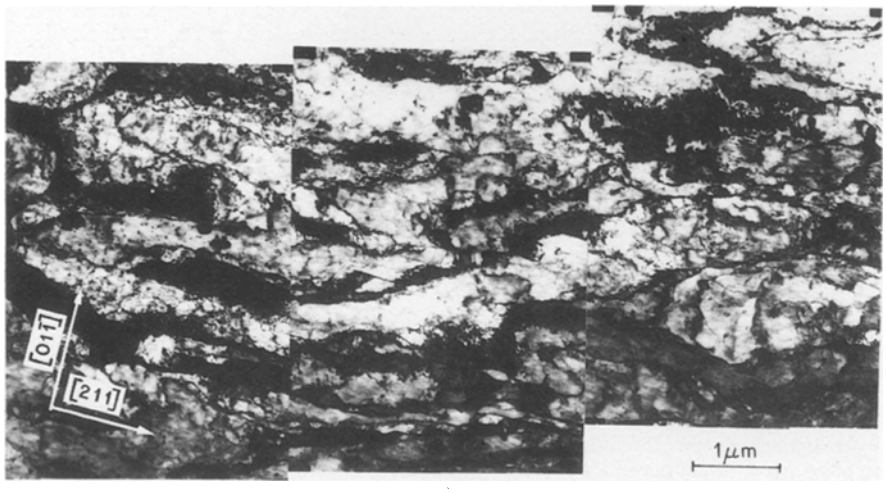

Figure 5 Typical dislocation distribution observed in HSLA steel after cycling up to 12%.

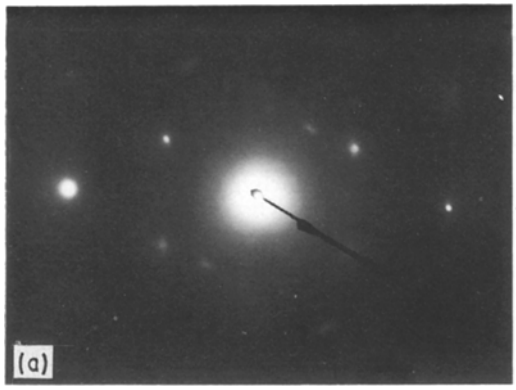

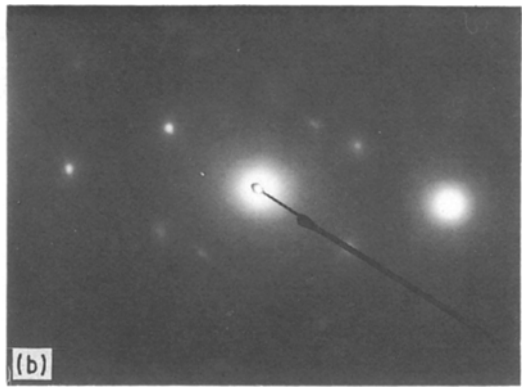

Figure 6 Selected area diffraction patterns, (a) and (b), of maximum misorientation taken from the area associated with Fig. 5; (c) geometry for evaluation of misorientation angle. (d^{Fe}_{121} $=0.117$ nm, $\lambda \approx 0.0037$ nm, $d^*_{12\bar{1}} = 1/d_{1\bar{2}1} \simeq 8.55\ \text{nm}^{-1} \equiv 0.036$ m, $(1/2)\ \alpha/2 = \sin^{-1}[(1/2)d^*_{121}/(1/\lambda)] = 0.905$, $\alpha = 3.6°$).

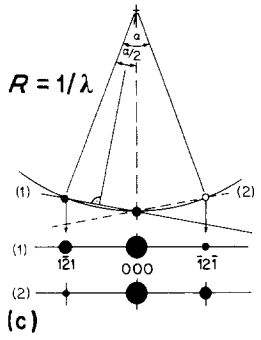

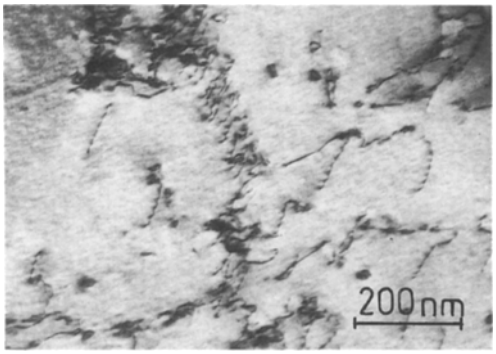

Figure 7 The dislocation distribution in a subcell wall.

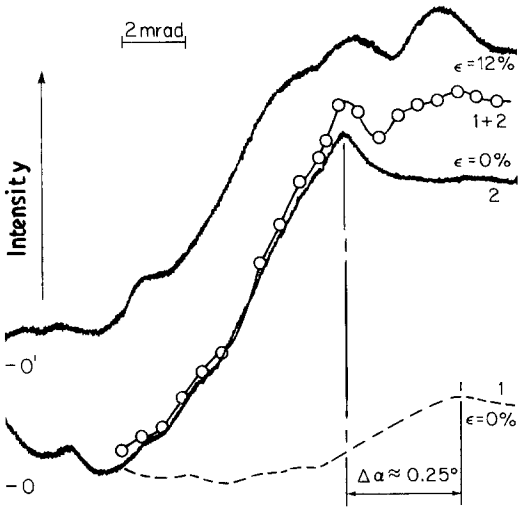

Figure 9 Comparison of the microdensitometer trace of an intensity distribution as taken from an ECP of a deformed grain with that graphically constructed by superposition of microdensitometer traces from the same but undeformed grain. (– – – 0.25 intensity and shifted microdensitometer trace, —— total calculated microdensitometer trace).

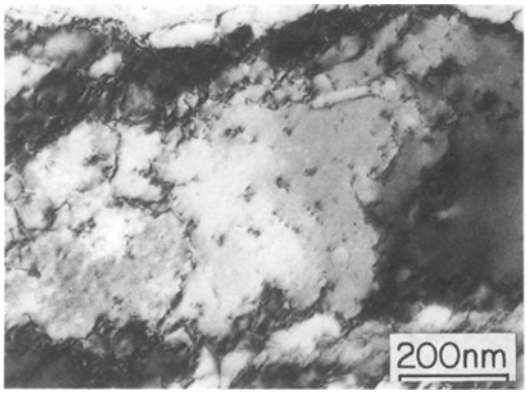

Figure 8 An example of single dislocations in the interior of a subcell.

observations that $l_s \sim 35$ nm and $b = 0.25$ nm, this gives $\alpha \sim 7.14 \times 10^{-3}$ rad $= 0.4°$. This value is rather typical for subcell misorientations and is quite close to that evaluated from the sketch in Fig. 9.

This is, however, an oversimplified model and does not include at least two important contributions. One of them concerns the dislocations inside the subcells and it is clear that their influence on broadening of the SACP lines is an obvious function of their density. The second one, and probably the more important, is linked with the ratio between the space occupied by subcell walls and that completely free of dislocations. Here we have to distinguish between two aspects. One of them concerns the "thickness" of the subcell walls, i.e. the range of the strain field exerted by dislocations grouped in the wall. The next is strictly connected with the number of the walls included inside the sampled volume, thus, if the dislocations in the walls are close enough such that their strain fields overlap, then this region would produce a strong decollimation of the Bloch wave. In this case, the influence will also depend on the "efficiency" of nonelastic scattering by this region [16–18]. The number of subcell walls included in the sampled region appears to be different, depend-

ing on their orientation with respect to the specimen surface. Two different orientations are shown in Fig. 10a and b. If it is assumed that the decollimation of the beam caused by inelastic scattering is proportional, e.g. to the projection of the subcell walls on the plane perpendicular to the optical axis, then there is no question that the probability of inelastic scattering in the case shown in Fig. 10b would be higher than that illustrated in Fig. 10a. From detailed calculations given in the Appendix, it follows that the ratio of the volume occupied by the strained region spread out around the subcell walls to the total volume being sampled is equal to ~ 0.17 and ~ 0.26 in Cases 1 and 2 (Fig. 10a and b, respectively). It means that SACP degradation will be sensitive to the orientation of these subcell walls. This would mean that for the same deformation level, the ECP line resolution would still be a function of the cell wall orientation. Several examples can be seen in Fig. 11a and b which show the SACPs from two differently oriented grains which had undergone almost the same deformation of 11%. Even a very rough comparison of the SACPs by eye allows one to conclude that the higher "quality" ECP pattern in presented in Fig. 11a. This can be documented noting a good visibility of fourth-order 220 bands. It should also be taken into account that different lines have a different sensitivity to deformation because of strain anisotropy [19]. The relatively small penetration depth of the electron beam during electron channelling [20–22] means that the wall-orientation effect mentioned above should not be overestimated.

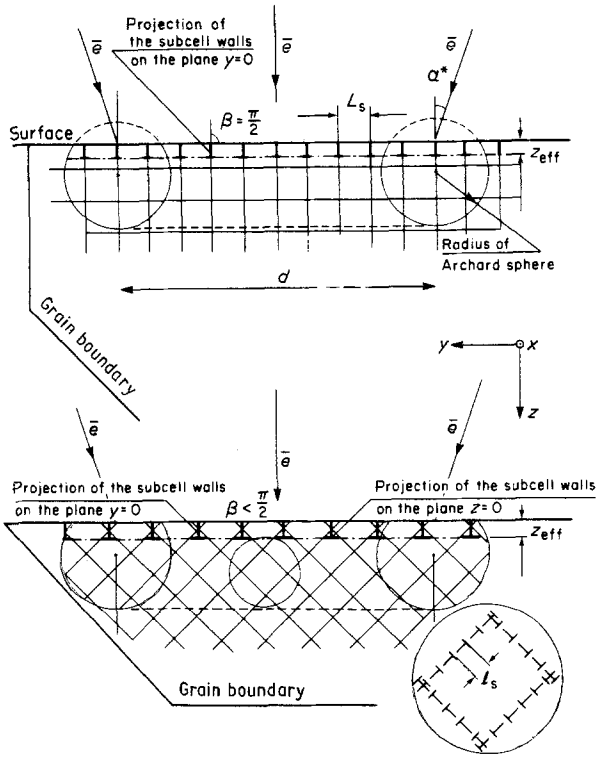

Figure 10 Two different orientations of a subcell system sampled by the rocking beam, (a) "cubic" subcells orientated perpendicular to the surface, (b) "cubic" subcells tilted with respect to the surface. (d is the diameter of rocking beam $\approx 10\,\mu m$, L_s is the subcell size $\sim 1\,\mu m$, z_{eff} the effective depth of penetration (order of $150\,nm^{-1}$ for $U = 25\,kV$, α^* is the rocking angle)

All of these effects can produce a large scatter in the experimental results [23]. Finally, Stickler *et al.* [6] had previously pointed out a need for studying the relationships between the ECP-line resolution and dislocation distribution. They presented three different curves representing a correlation between the pattern line resolution and deformation for three different materials, characterized by a different distribution of dislocations. Nickel, which had the dislocations arranged in the form of subcells, exhibited a much smaller decrease of the ECP-line resolution with increasing dislocation density than Discalloy which possessed the dislocations distributed randomly. Consider their equation for relating line resolution, w (mrad), to dislocation density, ρ (cm^{-2}), as given by

$$w = A \log \rho + B \qquad (1)$$

where, ρ is the dislocation density and A, B constants equal to 3 and -24, respectively. If this is applied to our data, then in the present experiment, w should be equal to 5.71 mrad. This value is much smaller than the observed value which was equal to 8.15 mrad. For the latter line resolution the dislocation density should be $5.2 \times 10^{10}\,cm^{-2}$ ($5.2 \times 10^{14}\,m^{-2}$). Such a discrepancy between that and the observed value of $8 \times 10^{13}\,m^{-2}$ appears to be too large to be explained by any artifact of counting in thin foils. It seems reasonable to explain this by the subcells having a specific distribution of dislocations with low-energy

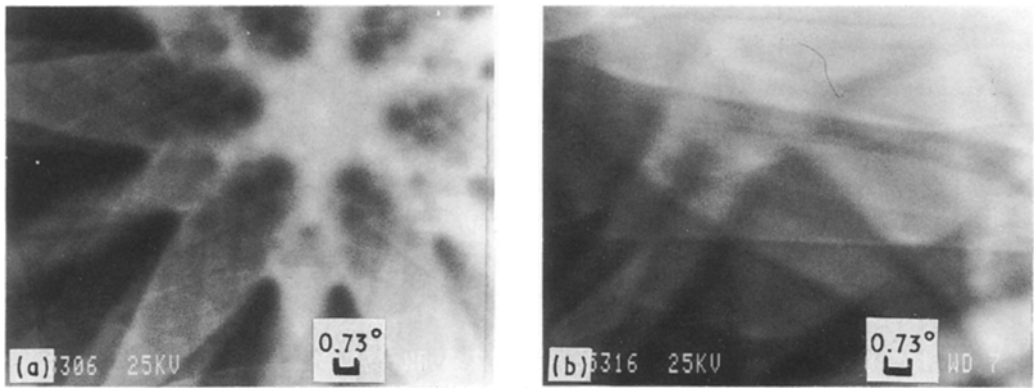

Figure 11 ECP lines from two different oriented grains, (a) and (b), which experienced nearly the same deformation by cycling.

configurations. It has been calculated that dislocations placed in the subcell wall, separated by a distance l_s, do exert a long-range stress field when under an external stress [23]. In the relaxed state, however, these low energy configurations have a much reduced effect on lattice bending, thus the total deformed part of the crystal is much less than if dislocations were distributed randomly. It follows that the probability of decollimation of a Bloch wave as a result of interaction with the deformed body is much less and therefore degradation of SACPs will be smaller. According to our most recent results, the functions describing the relationship between deformation, ε, and the SACP-line degradation, m, in the case of tension and fatigue can be represented by Equations 2 and 3 respectively [24]

$$m_1 = 1.0 + A_1\varepsilon \quad (2)$$

$$m_2 = 1.0 + A_2\varepsilon^n \quad (3)$$

where A_1 and A_2 are 0.059 and 0.0836, respectively, and $n \sim 0.7$, thus, for a given strain, $m_2 \leqslant m_1$, the effect being greater at larger strains.

We are aware that the results presented herein do not provide a quantitative analysis of the direct relationship between the line widths and deformation level. Nevertheless, the results have suggested several reasons for the sometimes surprising results that have been reported and have also explained why in the case of the subcell structure that the width of SACP lines are usually smaller than what would be expected from randomly arranged forest dislocations.

6. Conclusions

The conclusions are as follows.

(1) The SACP-line resolution not only depends on the total density of dislocations but also on their distribution.

(2) For a given density of dislocations, the degradation of SACPs is more for a random distribution than one with a low-energy subcell structure.

(3) The arrangement of the dislocations into subcells makes the body a two-component medium in which the spaces almost free of dislocations (undeformed) are penetrated by a high density dislocation array forming a three-dimensional network of subcell walls. From the point of view of SACP formation such a structure will generate an image by superposition of ECPs from relatively undeformed regions. The intensity profiles are thus shifted each from the other by an angle α which is a function of subcell misorientation.

(4) In the present study of subcell structures, the increase in the width of ECP-lines is mostly influenced by the value of $\pm \Delta\alpha$ which can be considered as a scattering band for an average misorientation typical for a given density of dislocations.

Acknowledgements

The authors would like to acknowledge support from the office of Basic Energy Sciences, Materials Science Division of the US Department of Energy under Contract No DE-FGO2-84ER45141, and Ms Lynn Seifried for technical assistance.

Appendix: Calculations of the relative volume occupied by distorted regions as a function of subcell orientation

The main assumption is that the probability of a Bloch wave being decollimated depends on the number of non-elastic scattering events. This in turn is a function of how often an electron meets a distorted region. It follows from these that degradation of SACP-lines should be proportional to the relative volume occupied by these disturbing regions which as we noted before depends on the orientation of subcell walls in the sampled volume (Fig. 10a and b). Calculations below only concern the central part of the sampled volume dimension of d length, L_s width and z_{eff} thickness where z_{eff} is the effective penetration depth [22]. Consider cubic subcells of an edge, L_s, inclined only in the plane perpendicular to the specimen surface, i.e. one set of walls is parallel to that surface. The details of this simplified geometry are shown in Fig. A1. First, start by evaluating the total surface included in the considered volume.

Case 1. $\beta = \pi/2$

$$S_1 = n_x S_x + \frac{1}{2}2S_y = \frac{d}{L_s}L_s z_{eff} + dz_{eff} = 2dz_{eff} \quad (A1)$$

where n_x is the number of the walls perpendicular to the x-axis equal to d/L_s, S_x the unit surface of the wall equal to $L_s z_{eff}$ and S_y the total surface of the walls lying in the plane perpendicular to the y axis, equal to dz_{eff}.

Case 2. $\beta < \pi/2$

$$S_2 = n_a S_a + n_b S_b + \frac{1}{2}S_y \quad (A2)$$

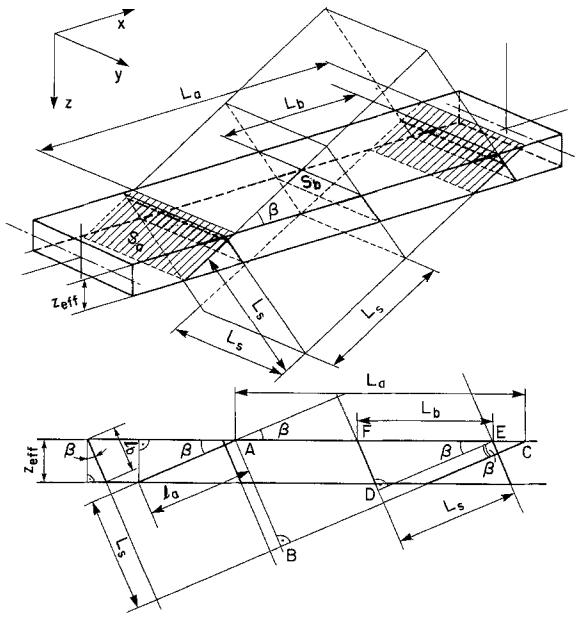

Figure A1 Details of geometry for evaluation of the relative space occupied by the subcell walls.

where n_a and n_b the number of walls of the unit surface, S_a and S_b, respectively.

$$n_a = d/L_a \quad \text{and} \quad n_b = d/L_b \qquad \text{(A3)}$$

From the triangles ABC and DEF, it follows that

$$L_a = L_s/\sin\beta \quad \text{and} \quad L_b = L_s/\cos\beta \qquad \text{(A4)}$$

In turn

$$S_a = L_s l_a \quad \text{and} \quad S_b = L_s l_b \qquad \text{(A5)}$$

where

$$l_a = z_{eff}/\sin\beta \quad \text{and} \quad l_b = z_{eff}/\cos\beta \qquad \text{(A6)}$$

By substituting Equations A3 to A6 into A2, it follows that

$$S_2 = \left(\frac{d}{L_s}\sin\beta\right)L_s\frac{z_{eff}}{\sin\beta} + \left(\frac{d}{L_s}\cos\beta\right) \times L_s\frac{z_{eff}}{\cos\beta} + dz_{eff} = 3dz_{eff} \qquad \text{(A7)}$$

To convert this into volume we need to assume the "thickness" of the disturbing region spread out around the subcell walls. According to Li [25], dislocations placed in the subcell wall, separated by a distance l_s, cause an annihilation of the long-range stresses which does not exceed $\pm l_s$. Assume then that the "thickness" of the disturbed region is $\delta = \pm l_s$. From TEM observations we measured $l_s \approx 35$ nm which means $\delta = 0.07$ μm. If we now assume $L_s = 0.8$ μm and $z_{eff} = 0.05$ μm, $d = 10$ μm, then

$$V_1 = S_1\delta = 210 \times 0.05 \times 0.07 \simeq 0.07\ \mu m^3$$

and

$$V_2 = S_2\delta = 3 \times 10 \times 0.05 \times 0.07 \simeq 0.105\ \mu m^3$$

Since the total volume being sampled $V_t = dL_s z_{eff} = 0.4\ \mu m^3$, then

$$V_1/V_t \simeq 17.5\% \quad \text{and} \quad V_2/V_t \simeq 26.2\%$$

It follows that the "density" of the disturbed region is a function of orientation of the subcell walls. For the case considered above, the volume occupied by the subcells inclined at some angle $\beta \ll \pi/2$ is $\sim 50\%$ higher than in the case $\beta = (\pi/2 + \beta_{cr})$. The value of β_{cr} depends on the diameter of the sampled area and the effective thickness, z_{eff}, according to the formula

$$\beta_{cr} = \tan^{-1}(z_{cr}/d) \qquad \text{(A8)}$$

which for the assumptions given before is equal to about 0.3°. In the special case when the subcell walls at the bottom are inside the sampled volume, i.e. $(\pi/2) - \beta_{cr} < \beta < (\pi/2) + \beta_{cr}$. Then the relations would be opposite which means that $V_1 = S_1\delta + L_s d\delta = 0.63\ \mu m^3$ and hence the ratio $V_1/V_2 \approx 6$. Since $V_1/V_t \approx 0.6$ it may suggest that such situations will be close to a random distribution of dislocations. For this case it can be assumed that the ratio between the disturbing volume versus the sampled one is equal to 1.

References

1. D. G. COATES, *Phil. Mag.* **16** (1967) 1179.
2. D. L. DAVIDSON, *J. Mater. Sci. Lett.* **1** (1982) 236.
3. W. W. GERBERICH and E. KURMAN, *Scripta Metall.* **49** (1985) 295.
4. D. L. DAVIDSON, *Scanning Electron Microscopy* **1** (1977) 431.
5. "Scanning Electron Microscopy/I" *Idem* **373**, edited by O. Johari (JLL. IITRI, Chicago, 1984).
6. R. STICKLER, C. W. HUGHES and G. R. BOOKER, Proceedings of the 4th Annual SEM Symposium, edited by O. Johari (IITRI, Chicago, 1971) pp. 475–480.
7. R. STICKLER and G. R. BOOKER, in "Electron Microscopy and Structure of Materials", (University of California, Berkeley, 1972).
8. A. W. RUFF, *Wear* **40** (1976) 59.
9. D. L. DAVIDSON, Proceedings of the 7th Annual SEM Symposium, edited by O. Johari (IITRI, Chicago, 1974) pp. 927–934.
10. W. W. GERBERICH, A. G. WRIGHT, E. KURMAN and K. A. PETERSON, "Fracture Measurements of Localized Deformation by Novel Techniques", edited by W. W. Gerberich, and D. L. Davidson, (TMS-AIME, Warrendale, PA, 1985) pp. 59–74.
11. D. C. JOY, D. E. NEWBURG and D. L. DAVIDSON, *J. Appl. Phys.* **53** (1982) R-81-R-122.
12. P. B. HIRSCH and C. J. HUMPHREYS, Proceedings of the 3rd Annual SEM Symposium, Chicago, edited by O. Johari (IITRI, Chicago, 1970) pp. 449–455.
13. D. HULL, "*Introduction to Dislocation*," 2nd Edn (Pergamon, Oxford, 1975).
14. S. NAKAGAWA, *JEOL News* 24E-17, 7 (1986).
15. M. KACZOROWSKI, unpublished results.
16. H. E. BISHOP, in "Quantitative Scanning Electron Microscopy", edited by D. B. Mott, M. D. Muir, P. R. Grant and J. M. Boswarra, (Academic Press, London, 1974) p. 41.
17. L. REIMER, in "Transmission Electron Microscopy, Physics of Image Formation and Microanalysing," (Springer Berlin, 1984) p. 135.
18. Y. T. GOLDSTEIN, D. E. NEWBURY, P. ECHLIU, D. C. JOY, C. FIROR and F. LIFSHIU, in "Scanning Electron Microscopy and X-Ray Microanalysis", (Plenum, New York, 1981) p. 53.
19. D. L. DAVIDSON, *Int. Met. Rev.* **29** (1984) 75.
20. J. A. ABROYAN and D. A. PODSVIROV, *Pis'ma Zh. Tekn. Fiz.* **7** (1981) 181.
21. T. YAMAMOTO, *Phys. Status Solidi* **44** (1977) 467.
22. M. KACZOROWSKI and W. W. GERBERICH, *Mater. Sci. Lett.* (1986) 244.
23. J. C. GIBELING and W. D. NIX, *Acta Metall.* **28** (1980) A743.
24. M. KACZOROWSKI and W. W. GERBERICH, *Scripta Metall.* **20** (1986) 1597.
25. J. C. M. LI, in "Electron Microscopy and Strength of Crystals", (Wiley, New York, 1963) p. 713.

Received 3 October 1989
and accepted 9 April 1990